Nuclear Instruments and Methods in Physics Research A 634 (2011) S156–S160

Contents lists available at ScienceDirect

Nuclear Instruments and Methods in Physics Research A

journal homepage: www.elsevier.com/locate/nima

The performance of magnetic lens for focusing VCN-SANS

M. Yamada [a,*], Y. Iwashita [a], T. Kanaya [a], M. Ichikawa [a], H. Tongu [a], S.J. Kennedy [b], H.M. Shimizu [c], K. Mishima [c], N.L. Yamada [c], K. Hirota [d], J.M. Carpenter [e], J. Lal [e], K. Andersen [f], P. Geltenbort [f], B. Guerard [f], G. Manzin [f], M. Hino [g], M. Kitaguchi [g], M. Bleuel [h]

[a] ICR, Kyoto University, Gokasho, Uji, Kyoto 611-0011, Japan
[b] Bragg Institute, ANSTO, PMB#1, Lucas Heights, NSW 2234, Australia
[c] KEK, 1-1, Oho, Tsukuba, Ibaraki 305-0801, Japan
[d] RIKEN, 2-1, Hirosawa, Wako, Saitama 351-0198, Japan
[e] Argonne National Laboratory, IL 60439, USA
[f] ILL, 6 Rue Jules Horowitz, B.P.156, F-38042 Grenoble Cedex 9, France
[g] KURRI, 2-1010, Kumatori, Osaka 590-0494, Japan
[h] Reactor institut Delft TU Delft, Mekelweg 15, 2629 JB Delft, The Netherlands

NOP Collaboration

ARTICLE INFO

Available online 30 June 2010

Keywords:
Focusing lens
Permanent magnet
Pulsed neutron beams
Time of flight
Focusing VCN-SANS

ABSTRACT

We have developed a prototype rotating-permanent magnet sextupole lens (named rot-PMSx) for more efficient experiments with neutron beams in time of flight (ToF) mode. This lens can modulate the focusing strength over range $1.5\times10^4\,\mathrm{T/m^2}\leqslant g'\leqslant 5.9\times10^4\,\mathrm{T/m^2}$. Synchronization between the modulation and the beam pulse produces a focused beam without significant chromatic aberration. We anticipate that this lens could be utilized in focusing small angle neutron scattering (SANS) instruments for novel approach to high resolution SANS.

We carried out experiments testing the principle of this lens at the very cold neutron (VCN) beamline (PF2) at Institut Laue-Langevin (ILL), France. The focused beam image size at the detector was kept constant at the same beam size as the source (≈ 3 mm) over a wavelength range of $30\,\text{Å}\leqslant\lambda\leqslant 48\,\text{Å}$ in focal length of ≈ 1.14 m. The flux gain was about 12 relative to a beam without focusing, and the depth of focus was quite large. These results show the good performance of this lens and the system. Thereupon we have demonstrated the performance of this test bed for high resolution focusing of VCN-SANS for a well-studied softmatter sample; a deuterium oxide solution of Pluronic F127, an $(PEO)_{100}(PPO)_{65}(PEO)_{100}$ tri-block copolymer in deuterium oxide. The results of the focusing experiment and the focusing VCN-SANS are presented.

1. Introduction

We are developing a magnetic lens whose focusing strength can be modulated for focusing pulsed white neutron beams without significant chromatic aberration for application to time of flight (ToF) experiments [1,2]. The neutron beam flux is increased by this lens while the focusing preserves the two-dimensional symmetry. We named this lens rot-PMSx, an acronym for rotating Permanent Magnet Sextupole. This lens has other features; the focused beam is better defined than one focused by a material lens [3], the beam is always polarized and the focusing power is suitable for the neutrons which have energy less than that of cold neutrons (CN). Considering these features, we anticipate a niche for this lens in focusing small angle neutron scattering (F-SANS).

Furthermore, especially when we utilize very cold neutron (VCN) beams, this instrument has other advantages depending on the optical setup. The detector focus setup brings about a better resolution measurements, in other words, it is easier to reach smaller q-minimum and to provide better q-resolution while the instrument size is more compact than conventional pinhole-SANS instruments. These features are good for studying nano-materials, magnetism and so on. On the other hand, the sample focus setup is also feasible and efficient because the scattering angle is no longer small for VCN, that is to say, small or thin samples of protein or bio-samples are also measurable in the smaller q region. This is our novel approach for high resolution SANS named focusing VCN-SANS.

* Corresponding author.
E-mail address: yamada@kyticr.kuicr.kyoto-u.ac.jp (M. Yamada).

0168-9002/$ - see front matter © 2010 Elsevier B.V. All rights reserved.
doi:10.1016/j.nima.2010.06.259

We fabricated the prototype rot-PMSx and modified it in some points. We carried out the first focusing experiment with VCN in 2008 [2] at the VCN beamline (PF2) at Institut Laue-Langevin (ILL) [4], France and confirmed the focusing for selected neutron wavelengths and field strengths operating in ToF mode. In the second step, we carried out experiments to prove the principle of focusing neutrons without significant chromatic aberration over a wide neutron wavelength range. These results are presented together with the focusing principle of rot-PMSx in this document. The successful results with the focusing experiment led us to the next step; the demonstration of high resolution focusing VCN-SANS with rot-PMSx. To determine the performance of this system, we carried out a SANS experiment in ToF mode for a well studied softmatter sample; a 15 wt% deuterium oxide (D_2O) solution of Pluronic F127, which is composed of a poly(oxyethylen–oxypropylene–oxyethylen) ($PEO_{100}PPO_{65}PEO_{100}$) tri-block copolymer at 28 °C. Preliminary results for the Pluronic F127 are presented as well.

2. Focusing pulsed white neutron beams without significant chromatic aberration

The beam axis is defined as z-axis and the horizontal axis and the perpendicular axes in the transverse plane as x- and y-axis, respectively. The source of focusing power is the interaction between neutron's magnetic dipole moment and the magnitude of sextupole magnetic field described as

$$|\boldsymbol{B}_{\mathrm{sxt}}| = \tfrac{1}{2}g'(x^2+y^2). \quad (1)$$

The sextupole magnetic field strength corresponds to a positive constant value g'. In a sextupole magnetic field, neutrons which have spin parallel to the field are focused to the focal point and the others are defocused. The focal length Z_f is given by [13]

$$Z_f = Z_m + \frac{h}{\omega m_n \lambda}\cot\left(\frac{\omega m_n \lambda}{h} Z_m\right) : \omega^2 = g'|\mu_n/m_n| \quad (2)$$

where h, μ_n, m_n, Z_m, are Planck's constant, the mass and magnetic dipole moment of neutron, and the magnet length along the z-axis, respectively. The spin direction follows the magnetic field direction during the flight when the adiabatic condition [12] is fulfilled or the ambient magnetic field is strong and changes slowly. Beams should be polarized upstream of the lens in order to suppress the background from the defocused neutrons. Therefore, the focused beam is always polarized (with a loss of half of the neutrons of an incident beam).

The time variation of wavelength at the rot-PMSx lens is proportional to the time of flight, and then g' required to be modulated proportional to the t^{-2} to keep the focal length (Eq. (2)) constant independent from λ. The lens is composed of two concentric permanent magnet arrays, in sextupole geometry and so-called extended-Halbach type configuration [1,9–11] in order to generate the strong magnetic field. All of the magnets in this lens are made of NEOMAX [14]. The inner array has 6 poles made of laminated Permendur (Fe49-Co49-V2), which has the highest magnetic flux density among available soft magnetic materials. The sinusoidal modulation of g' is provided by rotating the outer array about the fixed inner array. We utilize the downward slope of the sinusoidal modulation to the beam pulse. When this modulation is synchronized with the beam pulse, the beam size is kept constant over a wide wavelength range. In our compact prototype of rot-PMSx the bore is ϕ15 mm, the magnet length is 66 mm, the modulation of g' covers the range $1.5\times10^4\,\mathrm{T/m^2} \le H \le 5.9\times10^4\,\mathrm{T/m^2}$, and the repetition rate of g' modulation is $\nu \le 25$ Hz. The outer array is driven by a 1.5 kW electric motor, through a belt drive.

3. Experiment

After some fine tuning on the rot-PMSx, we carried out the focusing experiment with the outer array rotating and with continuous modulation at the PF2-VCN beam line, ILL, equipped with a chopper to enable ToF measurements. This experiment had two purposes; as a proof-of-principle experiment of the focusing ability of this modulating magnetic lens' without significant chromatic aberration, and in preparation of a good test bed for demonstrating focusing VCN-SANS. To find the optimum delay between the magnetic field modulation and the chopper pulse for this setup, we first carried out a scan of the synchronization delay. Then we varied the detector position at the optimum delay to measure the depth of focus as well. After we optimized the performance of the system, we performed a focusing SANS experiment for a standard softmatter sample, Pluronic F127.

3.1. Experimental setup

The experimental setup is shown in the Fig. 1. The rot-PMSx is operated by a driving motor, the overall size of which is compact: the plate underneath the motor is 370 × 300 mm and the height is 435 mm.

The continuous VCN beam from the reactor is pulsed by the disc chopper located just after the exit of the neutron guide, rotating with 60 ms period. The beam is reflected and polarized by a magnetic supermirror that has $m=2.3$ with incident angle 6.8°. Only those neutrons which have spin parallel to the mirror's field are reflected and others go through the mirror to an absorber layer. This mirror also plays the role of a higher energy neutron filter, cutting off neutrons whose wavelengths are less than 30 Å to avoid the frame overlap. In this experiment, we did not use a filter for lower energy neutrons because their intensity was assumed to be small enough to ignore.

The source and the second collimator are $\phi_1 = 3$ mm and $\phi_2 = 14$ mm pinholes, respectively. Both are made of Cd plates. The second aperture is fixed on the front surface of the rot-PMSx. The beam focused by rot-PMSx is observed in the two-dimensional position sensitive detector called bidim80 [15], MSGC in Fig. 1. We selected the wavelength range of $30\,\text{Å} \le \lambda \le 48\,\text{Å}$ for this experiment.

Given the repetition rate of the VCN beam pulse and the wavelength range, we can calculate the reasonable focal length and the distance between the chopper and the detection point. Fig. 2 reveals the good conformity between the modulation of g' and beam pulse in the current setup: $Z_f = 1.14$ m and the distance from the chopper to the center of the lens $L_{tot} = 2.60$ m.

The significant distances between components are presented in Table 1. As can be seen in Table 1, the magnification of this optical arrangement is 1.0.

In order to conserve the spin polarization, a magnetic guide field of at least 50 Gauss is applied everywhere along the neutron flight path between the polarizing supermirror and the magnetic lens. The guide field was maintained by dipole and solenoid fields.

The times of flight of VCNs from the chopper to the detector are longer than for cold neutrons. The air molecules flying faster than the VCN, the scattering probability caused by the molecules increase proportional to the flight time, and thus the air scattering can no longer be ignored. Flight tubes filled with Helium gas were placed between the first collimator to the entrance of the rot-PMSx and from the exit of the rot-PMSx to the front of the detector. The pressure was slightly higher than atmospheric pressure. The first flight tube is equipped with the solenoid coil as a spin guide field.

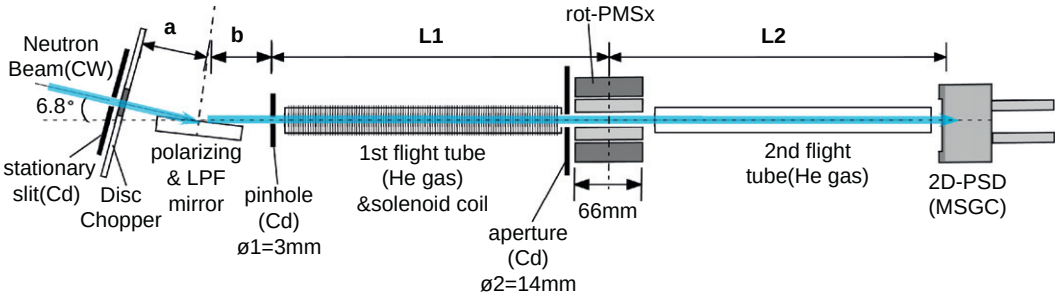

Fig. 1. The setup of the focusing experiment. The continuous beam from the reactor is pulsed and polarized. The source beam size is ϕ3 mm and we observed the focused beam size at a magnification of 1.0.

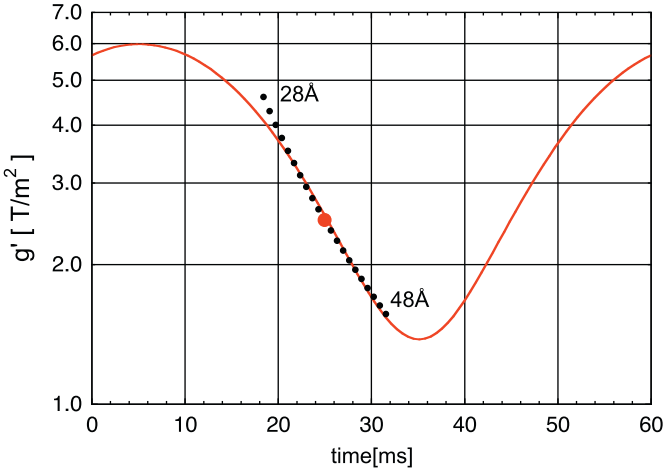

Fig. 2. The synchronization between the modulation of focusing power and the beam pulse obtained by calculation. The dotted line shows the required force to focus the pulsed beam at the rot-PMSx position. The solid line shows the field modulation of the rot-PMSx at the period 60 ms for a wavelength range 28 Å $\leq \lambda \leq$ 48 Å. With Z_f = 1.14 m, the distance between the chopper and the detection point is 4.88 m.

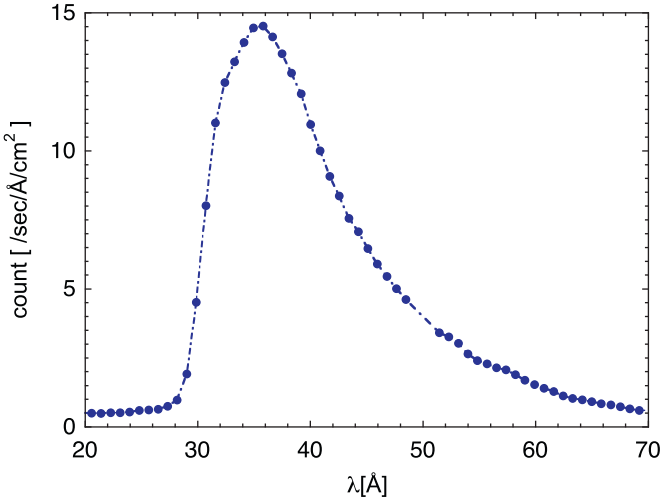

Fig. 3. The focused wavelength spectrum at the optimum delay and with the same setup as the delay scan measurement.

Table 1
Distances in the focusing measurements.

Chopper to pinhole through pol. mirror	**a** + **b**	325 mm
Pinhole to magnetic lens center	$\mathbf{L}_1$	2275 mm
Magnetic lens center to detector surface	$\mathbf{L}_2$	2275 mm
The focal distance	$2 \times Z_f$	2275 mm
Tof length L_{tot}		4875 mm

3.2. Results of the focusing experiment

We measured the x and y resolutions of the bidim80 as 3.3 and 2.0 mm, respectively. The observed beam profile was fitted by a two-dimensional Gaussian distribution function and we equated the beam size (FWHM) to $2 \times \sqrt{2\ln(2)\sigma^2}$, where σ^2 is the variance of the Gaussian.

3.2.1. The synchronization delay scan

The image size at the detector without the lens is 14.9 ± 2.6 mm over the wavelength range of 30 Å $\leq \lambda \leq$ 48 Å. With the sextupole lens in position and synchronized with the chopper the image size shrank to 3.0 $\pm$ 0.4 mm, as desired. The focused beam image size matches the source size (3 mm) over the wavelength range of 30 Å $\leq \lambda \leq$ 48 Å in focal length of $\approx$ 1.14 m. We measured the flux gain factor of the focusing system to be 12.4 larger than the system without the lens. This proves that the focusing performance of the rot-PMSx is consistent with the principle and that the chromatic aberration while focusing over a wide λ range is suppressed. We determined the optimum delay of 14 ms through the series of delay scans, as expected.

Fig. 3 shows the VCN beam spectrum that we measured at the detector position with the same setup as the delay scan measurement and with the optimum delay 14 ms. The peak wavelength is 36 Å.

3.2.2. The detector position scan

We also carried out a detector position scan to prove that the focal depth-of-field of the rot-PMSx is large for the sample focus setup. For example, focussed setups of SANS toward the small q's are limited by over-focused direct beam. Deep focal depth makes it easier to measure small samples in the small q-region. The range of acceptable focusing at the detector was up to 175 mm forward and 150 mm backward for the14-ms optimum delay (see Fig. 4). The beam sizes coincide each other remarkably well in our measurements, although we note a small increase in beam size with wavelength. This may indicate a slight mismatch between slope of g' and the neutron's time of flight.

To suppress beam loss caused by gravity, the beam is reflected upwards at the polarizing supermirror in Fig. 1 so that the beam current over whole wavelength range at the lens would become maximum. The measured aberrations caused by gravity at the detector position are represented by beam center (x_0, y_0) translations in Fig. 5, where the center for 30 Å was defined as (0, 0). The error bars represent only the chopper's opening time

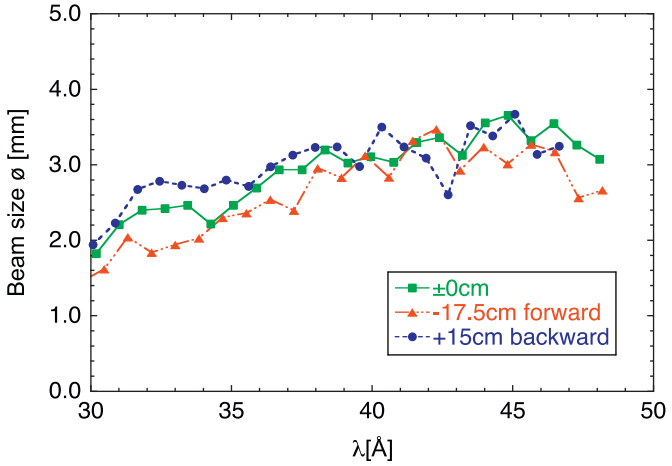

Fig. 4. The beam size at three detector positions. The solid triangles and circles represent the measurements at the maximum displacement 175 mm forward and 150 mm backward, respectively. The beam sizes without displacement (solid squares) are also plotted for comparison.

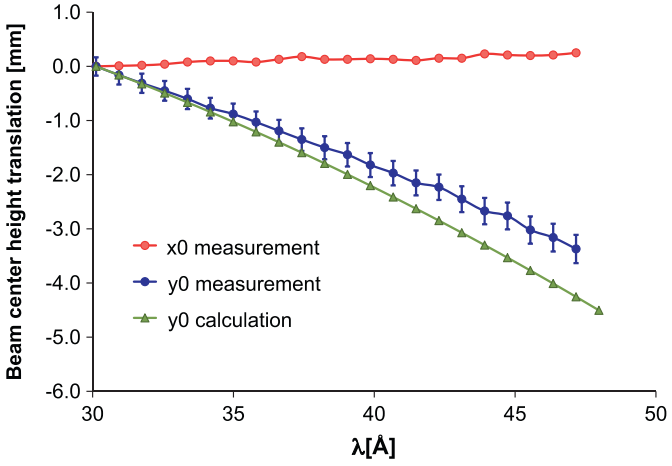

Fig. 5. The measured and simulated beam center translations at the detector position.

(1 ms) and detection bin width (1 ms). The estimated $\delta\lambda/\lambda$ in measured data in a time bin with 5 m flight path is $\lesssim 3\%$. (N.B. Since the chopper's opening time is 3 ms at the following SANS experiment and maximum $\delta\lambda/\lambda$ is 11%, the aberration caused by gravity is broader.) The aberration of vertical beam center y_0 cannot be ignored while the horizontal center x_0 is kept at the vicinity of 0. The discrepancy can be explained by taking beam distribution and detector resolution (ϕ1.5 mm) into account. Vertical geometry of a new design will relieve this problem.

3.3. Demonstration for focusing VCN-SANS

3.3.1. Pluronic F127

To determine the performance of this SANS instrument, we selected a well studied tri-block copolymer Pluronic F127, $((PEO)_{100}(PPO)_{65}(PEO)_{100})$. This polymer has been the subject of intense research because of its diverse phase transitions depending on both temperature and solution concentration [5,6] and is a commercially available nonionic macromolecular surfactant. At temperatures close to ambient, PPO part is no longer soluble in water and the unimer becomes amphiphilic. This results in self-aggregation into spherical micelles of Pluronic with the core

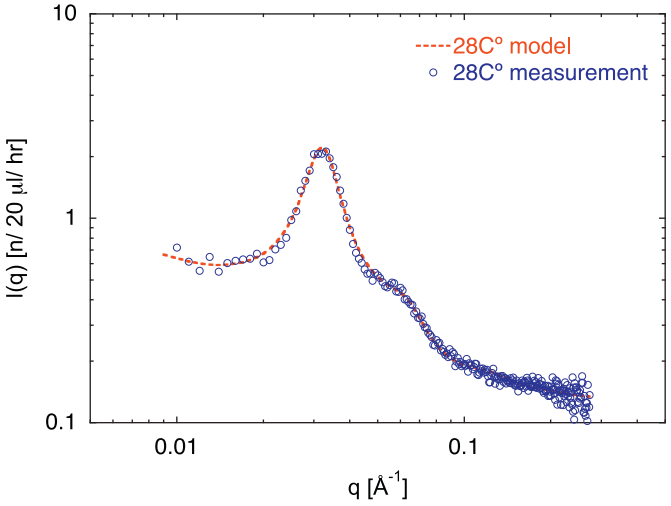

Fig. 6. The SANS plot for the Pluronic at 28 °C, with focused beam spectrum at the optimum delay and with the same setup as the delay scan measurement.

Table 2
The fitting parameters for the measurement of Pluronic (15 wt%).

Parameters	VCN-SANS (28.0 °C)
Tri-block radius of gyration R_g	12.8 Å
Micelle core radius R_c	46.2 Å
Micelle volume fraction ϕ	17.2%
Incoherent background I_{inc}	0.102 n/µl/h
Tri-block scattering factor	0.296 n/µl/h
Micelle scattering factor	6.59×10^{-12} n/µl/h

dominated by PPO and a corona dominated by the hydrated PEO blocks. Providing tri-block copolymers above typical concentration, the spherical micelles are close packed in a cubic phase. In this phase, the measured scattering intensity can be fitted to the model of Pedersen and Gerstenberg [7]. For calculation of the structure factor $S(q)$ the interaction potential is based on the hard sphere approximation [8]. The micelle form factor is assumed to follow a sharp interface of dense spherical objects. The scattered intensity has contributions from tri-block copolymers, the micelles, the micelle clusters, and the incoherent back ground. The function is determined by the polymers radius of the gyration R_g, the core radius R_c, the hard sphere volume fraction ϕ, and the incoherent background from the sample I_{inc}.

The structure factor is determined by the hard sphere volume fraction and two radii characteristic for the micelles; the core radius R_c and the hard sphere interaction radius R_{HS}, where $R_{HS} = 2 \times R_c$.

3.3.2. Results

The measurements were performed in ToF mode for 5 h and the sample-to-detector distance was just 100 mm. The sample was mounted in sealed quartz cuvette with 1 mm path length. Indicated by 26% transmission, multiple scattering of Pluronic was relatively high. However, since we had only limited time, we proceeded with measurements with this set up.

The measured scattering function $I(q)$ versus scattering vector q of 15 wt% Pluronic F127 at 28 °C per 20 µl/h is plotted in Fig. 6. It was fitted by the sum of the model of Pederson and Gerstenberg and Debye formula for Gaussian chains, and the results are listed in Table 2. These values are similar to those of the experiments performed by Mortensen and Talmon [5] or Prud'homme [6].

We note that the resolution of the measurement is really quite good, despite the compactness of the instrument. We also note that the background (I_{inc}) is relatively high, which may indicate a challenge for the application of VCN to SANS in hydrogenous media. This possibility will be explored in later experiments.

4. Conclusion

The results of the synchronization delay scan in focusing experiment proved that the performance of the prototype of rot-PMSx is exceptional. The wide wavelength range VCN beam over a range of $30\,\text{Å} \leq \lambda \leq 48\,\text{Å}$ are focused at the same focal point.

From the results of the detector position scan, we confirmed that the beam is focused in-between 175 mm forward and 150 mm backward, where the origin is the detector position in the delay scan. This system provides a special SANS setup: the beam focused at both points the sample and the detector as long as they are placed in-between the above range. The special setup allows user to measure smaller size samples at smaller q-region and with better resolution. After the focusing experiment, we moved on to the demonstration of the performance of this system for high resolution focusing VCN-SANS experiment for the tri-block copolymer Pluronic F127 in a compact geometry of just 5 m. All length scale variables and the micelle volume fraction are similar to the preceding experiments. These verify the quality of the experiment and the relevance of the model.

These encouraging results lead us to consider the new design of a focusing SANS system competitive with existing facilities by means of this novel approach utilizing the combination of lens and VCN. On the other hand, the remarkably dominated scattering scales (incoherent scattering background, and the scattering from micelles and tri-blocks) needs systematic total scattering cross-sections measurements in VCN region. The entirety of detailed results will be published soon.

Acknowledgments

This work is partially supported by the Japanese Ministry of Education, Science, Sports and Culture, Grant-in-Aid for Scientific Research(A), 18204023(2006) and 19GS0210.

References

[1] Y. Iwashita, et al., Nucl. Instr. and Meth. 73 (2007) 586.
[2] M. Yamada, et al., Physica B 404 (2009) 2646.
[3] S.M. Choi, et al., J. Appl. Crystallogr. 33 (2000) 793.
[4] PF2 beam line at ILL 〈http://www.ill.eu/instruments-support/instruments-groups/instruments/pf2/〉.
[5] K. Mortensen, Y. Talmon, Macromolecules 28 (1995) 8829.
[6] R.K. Prudfhomme, et al., Langmuir 12 (1996) 4651.
[7] J.S. Pedersen, M.C. Gerstenberg, Macromolecules 29 (1996) 1363.
[8] J.S. Pedersen, Adv. Colloid Interface Sci. 70 (1997) 171.
[9] CERN Courier, Int. J. High Energy Phys. 41(7) (2001) 9.
[10] M. Kumada, et al., IEEE Trans. Appl. Superconductivity AS-12 (1) (2002) 129.
[11] M. Kumada, et al., IEEE Trans. Appl. Superconductivity AS-14(2) (2004) 1287.
[12] H.M. Shimizu, et al., Nucl. Instr. and Meth. A 430 (1999) 423.
[13] J. Suzuki, et al., Nucl. Instr. and Meth. A 529 (2004) 120.
[14] NEOMAX 〈http://www.neomax-materials.co.jp/〉.
[15] B. Guerard, G. Manzin, Institute Laue Langevin, Private communication.